Kinetics of [Fe^{II}(edta)] Oxidation by Molecular Oxygen Revisited. New Evidence for a Multistep Mechanism

Sabine Seibig and Rudi van Eldik*

Institute for Inorganic Chemistry, University of Erlangen-Nürnberg, Egerlandstrasse 1, 91058 Erlangen, Germany

Received February 12, 1997[⊗]

A detailed mechanistic study of the reaction of [Fe^{II}(edta)] (edta = ethylenediaminetetraacetate) with molecular oxygen was conducted and the oxidation kinetics were investigated as a function of [Fe^{II}], [O_2], pH, temperature, and pressure. The observed kinetic data in the presence of an excess of [Fe^{II}(edta)] can be accounted for in terms of a four-step mechanism: reaction of (I) [Fe^{II}(edta)H_2O]$^{2-}$ with O_2 by a substitution-controlled process to form [Fe^{II}(edta)O_2]$^{2-}$; (II) electron transfer to form an Fe^{III}−superoxo species; (III) subsequent substitution on a second [Fe^{II}(edta)H_2O]$^{2-}$ anion followed by electron transfer to give [Fe^{III}(edta)−O_2^{2-}−Fe^{III}(edta)]$^{4-}$; and (IV) a fast decomposition yielding the monomeric [Fe^{III}(edta)]$^-$ and H_2O_2, which rapidly reacts with [Fe^{II}(edta)]. Rate and activation parameters for some of these steps are reported and discussed with reference to available literature data.

Introduction

There has been much interest in the oxidation of polyamino carboxylate complexes of Fe(II) by molecular oxygen and hydrogen peroxide over the past 4 decades.[1−12] The main interest in these reactions has resulted from their fundamental importance in biochemical processes, such as the cleavage of DNA, the decomposition of H_2O_2, and the dismutation of superoxide.[13−19] In this connection, we have previously studied the kinetics and mechanism of the autoxidation of Fe(II) induced through chelation by ethylenediaminetetraacetate (edta) and related polyamino carboxylate ligands.[20] Since then, a number of scientific and instrumental developments pertaining to this field have occurred, which encouraged us to revisit the autoxidation reaction of [Fe^{II}(edta)]. These include detailed structural information on complexes of [Fe^{II}(edta)] in the solid state[21,22] and the availability of sophisticated rapid-scan techniques and software packages that enable the analysis of multistep kinetic processes.

The present work describes a detailed kinetic study which could for the first time provide evidence for the occurrence of four subsequent reaction steps. These were studied as a function of concentrations, pH, temperature, and pressure. In addition, a number of experiments with radical scavengers using EPR techniques were performed in order to obtain further information on the nature of the redox products. A mechanism is presented that accounts for all spectroscopic and kinetic observations and is discussed with reference to earlier work reported in the literature.[4,6,7,10,12,20]

Experimental Section

Materials. Chemicals of analytical reagent grade and ultrapure water were used throughout this study. [Fe^{II}(edta)] was prepared in solution from $FeSO_4 \cdot 7H_2O$ and Na_4(edta) or H_4(edta). NaOH, $HClO_4$, and NaOAc were used to adjust the pH of the test solutions.[23] The ionic strength of the medium was adjusted with $NaClO_4$. The radical scavenger ATBS [2,2′-azinobis(3-ethyl-2,3-dihydrobenzthiazole-6-sulfonate)] was obtained from Aldrich. Hydrogen peroxide stock solutions were prepared from 30% hydrogen peroxide.

Preparation of Solutions. [Fe^{II}(edta)] is extremely oxygen-sensitive and rapidly oxidized to [Fe^{III}(edta)].[24] Test solutions were therefore prepared with the exclusion of oxygen in the following way: A stock solution of the ligand at the appropriate ionic strength was degassed and then saturated for 20 min with pure nitrogen. The appropriate amount of $FeSO_4 \cdot 7H_2O$ was then added. Finally, the pH was adjusted by addition of $HClO_4$ or NaOH using a glass electrode under the exclusion of oxygen. Oxygen-saturated solutions were prepared by bubbling air or O_2 through a solution for at least 20 min. The required O_2 concentration was obtained by diluting the solutions with nitrogen-saturated stock solutions. All solutions were freshly prepared before the measurements. The ionic strength was adjusted with $NaClO_4$ to 0.5 M for all solutions, and acetate buffer was employed for pH > 3. Test measurements showed that the acetate buffer had no significant

[⊗] Abstract published in *Advance ACS Abstracts,* August 1, 1997.

(1) Cher, M.; Davidson, N. *J. Am. Chem. Soc.* **1955**, *77*, 793.
(2) Huffman, R. E.; Davidson, N. *J. Am. Chem. Soc.* **1956**, *78*, 4836.
(3) Kaden, T.; Fallab, S. *Chelate Catalysed Autoxidation of Iron(II) Complexes*; Macmillan: New York, 1961.
(4) Kurimura, Y.; Ochiai, R.; Matsuura, N. *Bull. Chem. Soc. Jpn.* **1968**, *41*, 2234.
(5) Purmal, A. P.; Skurlatov, Y. I.; Travin, S. O. *Bull. Acad. Sci. USSR, Div. Chem. Sci. (Engl. Transl.)* **1980**, *29*, 315.
(6) Sada, E.; Kumazawa, H.; Machida, H. *Ind. Eng. Chem. Res.* **1987**, *26*, 1468.
(7) Brown, E. R.; Mazzarella, J. D. *J. Electroanal. Chem. Interfacial Electrochem.* **1987**, *222*, 173.
(8) Rahhal, M.; Richter, H. W. *J. Chem. Soc.* **1988**, *110*, 3126.
(9) Rush, J. D.; Koppenol, W. H. *J. Am. Chem. Soc.* **1988**, *110*, 1957.
(10) Wubs, H. J.; Beenackers, A. A. C. M. *Ind. Eng. Chem. Res.* **1993**, *32*, 2580.
(11) Liang, L.; McNabb, J. A.; Paulk, J. M.; Gu, B.; McCarthy, J. F. *Environ. Sci. Technol.* **1993**, *27*, 1864.
(12) King, D. W.; Lounsbury, H. A.; Millero, F. J. *Environ. Sci. Technol.* **1995**, *29*, 818.
(13) Krapp Pogozelski, W.; McNeese, T. J.; Tullius, T. D. *J. Am. Chem. Soc.* **1995**, *117*, 6428.
(14) Fontecave, M.; Pierre, J. L. *Bull. Soc. Chim. Fr.* **1993**, *130*, 77.
(15) McClune, G. J.; Fee, J. A.; McCluskey, G.; Groves, J. T. *J. Am. Chem. Soc.* **1977**, *99*, 5220.
(16) Bull, C.; McClune, G. J.; Fee, J. A. *J. Am. Chem. Soc.* **1983**, *105*, 5290.
(17) Hertzberg, R. P.; Dervan, P. B. *Biochemistry* **1984**, *23*, 3934.
(18) Youngquist, R. S.; Dervan, P. B. *J. Am. Chem. Soc.* **1985**, *107*, 5528.
(19) Dervan, P. D. *Science* **1986**, *232*, 464.
(20) Zang, V.; van Eldik, R. *Inorg. Chem.* **1990**, *29*, 1705.
(21) Mizuta, T.; Wang, J.; Miyoshi, K. *Bull. Chem. Soc. Jpn.* **1993**, *66*, 2547.
(22) Mizuta, T.; Wang, J.; Miyoshi, K. *Inorg. Chim. Acta* **1995**, *230*, 119.
(23) Perrin, D. D.; Dempsey, D. *Buffers for pH and Metal Ion Control*; Chapman and Hall: London, 1974.
(24) Ogino, H.; Nagata, T.; Ogino, K. *Inorg. Chem.* **1989**, *28*, 3656.

S0020-1669(97)00158-4 CCC: $14.00

effect on the observed kinetics. Test solutions were transferred to the stopped-flow unit by using gastight syringes.

Instrumentation. The kinetic experiments were performed on Biologic SFM-3 and Applied Photophysics SX.18MV stopped-flow units, to which an on-line data acquisition system was connected. Rapid-scan spectra were recorded with the aid of a J & M (Aalen, Germany) diode array detector, which was connected to an Applied Photophysics stopped-flow instrument, and also obtained from a combination of absorbance−time traces recorded over the investigated wavelength range. Kinetic measurements at pressures up to 120 MPa were performed on a homemade high-pressure stopped-flow unit.[25,26] UV−vis spectra were recorded on a Hewlett-Packard diode array spectrophotometer. The pH of the stock solutions was measured with the aid of a Mettler Delta 340 pH meter. The reference electrode was filled with NaCl instead of KCl to prevent precipitation of $KClO_4$. All kinetic traces were analyzed by using OLIS KINFIT (OLIS, Bogart, GA), IGOR PRO (Lake Oswego, OR), and Applied Photophysics Kinfit (Applied Photophysics Limited, Leatherhead, U.K.) software. For global analysis, spectra were recorded on the Applied Photophysics Instrument and fitted with the aid of the Applied Photophysics Software Package. EPR spectra were recorded on a Bruker ESP 300 at 75 K. The aqueous solutions were prepared as described above and then rapidly frozen in liquid nitrogen.

Results and Discussion

Spectral Observations. A number of experiments were performed with the spectrophotometric rapid-scan equipment in order to obtain information on the progress of the oxidation reaction when solutions of [Fe^{II}(edta)] were mixed with solutions containing dissolved oxygen. Typical spectra are shown in the Supporting Information (Figure S1), which indicate that both [Fe^{II}(edta)] and [Fe^{III}(edta)] exhibit an absorbance maximum at 260 nm and that the molar extinction coefficient for [Fe^{III}(edta)] is significantly higher than that for the [Fe^{II}(edta)] complex. The overall oxidation reaction is accompanied by a significant decrease in [H^+], which can be accounted for in terms of the following reaction:

$$O_2 + 4e^- + 4H^+ \rightarrow 2H_2O$$

Therefore acetate buffers, which had no influence on the kinetic measurements, were employed at higher pH values.[23]

The observed spectral changes indicated that the reaction of [Fe^{II}(edta)] with molecular oxygen can best be followed at 370 nm in the presence of an excess of [Fe^{II}(edta)] and at 260 nm in the presence of an excess of O_2 using a 1 cm cuvette. All kinetic traces were measured over more than 5 half-lives.

Kinetic Measurements. Kinetic traces recorded in the presence of excess [Fe^{II}(edta)] clearly showed a multistep process that could not be fitted by a single-exponential function. In most cases, the kinetic traces could be fitted to two exponential functions. There was also evidence for an additional reaction step occurring prior to these functions, which was in most cases accompanied by such a small absorbance change that it could not be resolved kinetically. However, at pH 2.2, this initial step could be resolved; a typically observed trace is shown in Figure 1a. The initial absorbance−time trace reminds one of an autocatalytic process, but addition of [Fe^{III}(edta)] to the test solution did not resolve the observed induction period. Kinetic traces recorded under these conditions could be fitted to two exponential functions. Similarly, kinetic traces recorded over longer reaction times (see Figure 1b) could also be fitted to two exponentials. Finally, the complete kinetic trace (see Figure 1c) could, with the aid of an iteration technique, be fitted to three exponential functions. The application of the mentioned software packages enabled the resolution of these traces, also under conditions where some reaction steps exhibit relatively small absorbance changes. Such a detailed analysis of the kinetic traces was not possible in our earlier study,[20] since the available software allowed only a single-exponential fit.

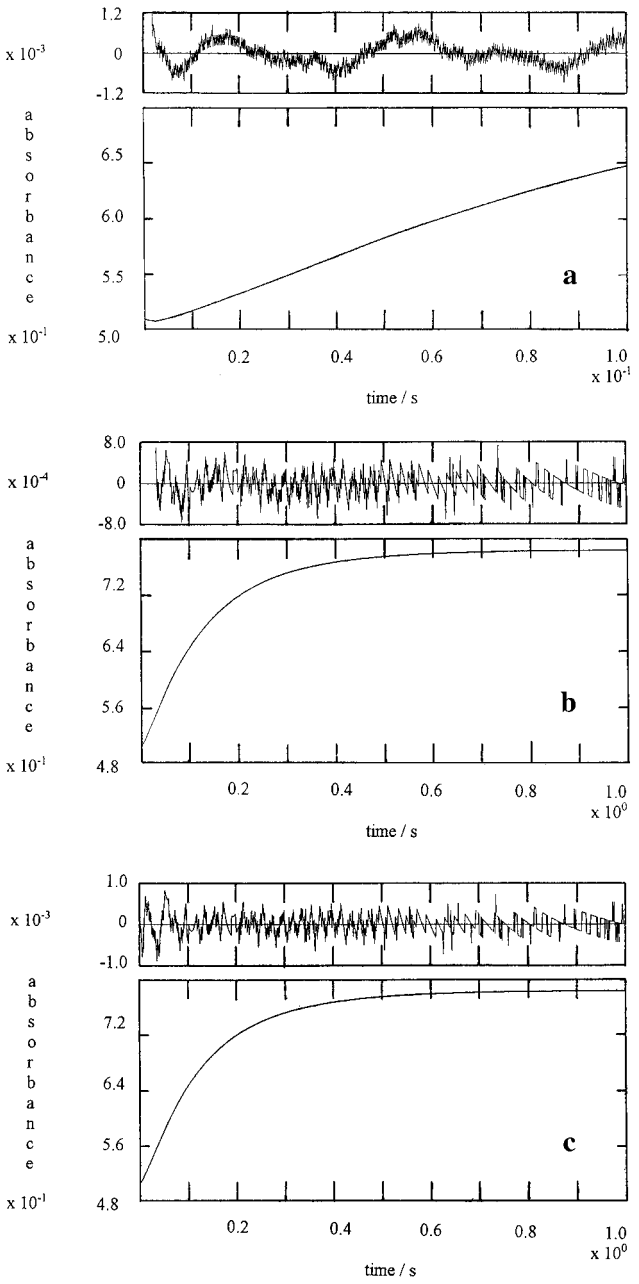

Figure 1. (a) Typical absorbance−time trace, including the first fast step: fit with two exponential functions. (b) Typical absorbance−time trace recorded over longer reaction time: fit with two exponential functions. (c) Absorbance−time, the same as in Figure 1b, but with the aid of an iteraction technique fitted with three exponential functions. Experimental conditions: [Fe^{II}(edta)] = 2×10^{-3} M, [O_2] = 1.25×10^{-4} M, ionic strength = 0.5 M, pH = 2.2, T = 25 °C, λ = 370 nm.

The pH dependence of the reaction in the presence of an excess [Fe^{II}(edta)] was studied in the pH 1−6 range, and the results obtained at 25 °C are summarized in Figure 2. Only the pH dependence of the two main reaction steps could be resolved because of our inability to resolve all the reaction steps over the entire pH range. The results reported in Figure 3 are in close agreement with the general trend observed previously.[20] Both observed steps show bell-shaped curves with a maximum between pH = 2.5 and pH = 3 and a pH-independent region at pH > 4. The obtained k_{obs} values for the two steps differ by

(25) van Eldik, R.; Palmer, D. A.; Schmidt, R.; Kelm, H. *Inorg. Chim. Acta* **1981**, *50*, 131.
(26) van Eldik, R.; Gaede, W.; Wieland, S.; Kraft, J.; Spitzer, M.; Palmer, D. A. *Rev. Sci. Instrum.* **1993**, *64*, 1355.

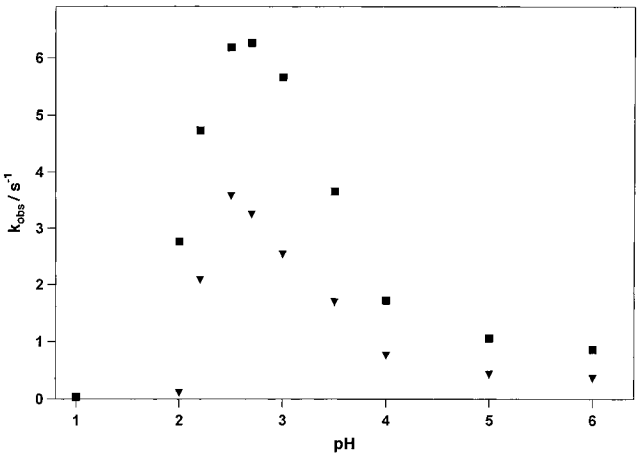

Figure 2. pH dependence of k_{obs2} (■) and k_{obs3} (▼) for the oxidation of [Fe^{II}(edta)] in the presence of an excess of [Fe^{II}(edta)]. Experimental conditions: [Fe^{II}(edta)] = 2.5×10^{-3} M, [O_2] = 1.25×10^{-4} M, ionic strength = 0.5 M, [acetate buffer] = 0.1 M for pH > 3, T = 25 °C, λ = 370 nm.

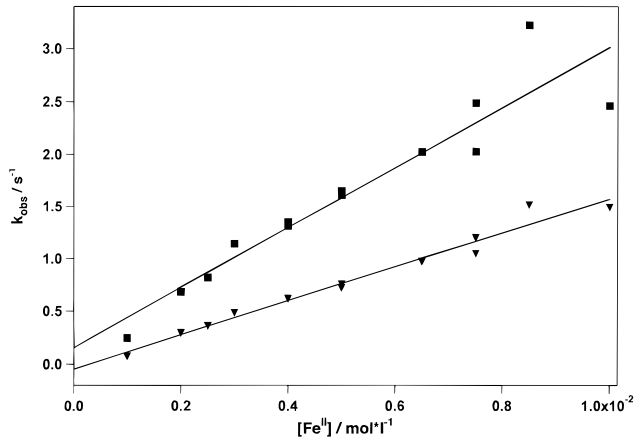

Figure 3. k_{obs2} (■) and k_{obs3} (▼) as a function of [Fe^{II}(edta)] for the oxidation of [Fe^{II}(edta)] at low [Fe^{II}(edta)]. Experimental conditions: [O_2] = 1.25×10^{-4} M, ionic strength = 0.5 M, [acetate buffer] = 0.1 M, pH = 6, λ = 370 nm.

about a factor of 2. The data for the faster reaction agree very closely with those reported for the previously observed single reaction step.[20] Our earlier analysis did not detect the initial step and the final slow step of the process mainly because these steps are accompanied by relatively small absorbance changes, which cause only minor deviations when a single-exponential fit is used. Important is our observation that both reaction steps reported in Figure 2 exhibit almost identical pH dependencies. pH titrations of [Fe^{II}(edta)] in the range pH 3−11[27] revealed no evidence for the deprotonation of a coordinated water molecule.

It is known from X-ray structural data that the complex, which was crystallized from neutral solution, exists as a seven-coordinate [Fe^{II}(edta)H_2O]$^{2-}$ species with a monocapped trigonal-prismatic geometry (MCP).[21] On acidification, the edta chelate can be protonated, to form a monoprotonated species [Fe^{II}(edtaH) H_2O]$^{-}$, which adopts a pentagonal-bipyramidal geometry (PB) in the solid state.[22] pK_a values of 3.0, 2.8, 2.5, and 2.1 for the protonation of the edta ligand have been reported in the literature.[4,27−29] The increase in k_{obs} with increasing [H^+] at pH < 5 could be associated with the protonation of the edta ligand, which results in a change in geometry from MCP to PB. The higher reactivity of the PB geometry could be due to the greater bite angle in the PB form such that the attacking oxygen molecule has more space to enter the coordination sphere and to substitute the coordinate water. Further acidification results in a diprotonation of the complex. This diprotonated form of the complex results again in a monocapped trigonal-prismatic geometry.[22] Furthermore the Fe−OH_2 bond is shortened here as a result of protonation of two acetate arms. The shorter Fe−OH_2 bond in this diprotonated complex could be responsible for the decrease in reactivity observed at pH < 2.5. It is quite realistic to expect that [Fe^{II}(edta)] has similar structures in solution and the solid state. For the [Fe^{III}(edta)] complex, it is known, for instance, from NMR and Raman studies,[30−34] that the structure in solution is the same as that in the crystalline state.[35−37] A typical speciation diagram based on potentiometric titration data[27] (see Supporting Information (Figure S2)) further supports the observed reactivity pattern.

In our earlier study,[20] we offered an alternative explanation since no information on the pH-dependent structure of [Fe^{II}(edta)] under such conditions was available at that stage. We therefore preferred to analyze the data in terms of an acid-catalyzed electron-transfer process during which [Fe^{II}(edta)O_2]$^{2-}$ is converted to [Fe^{III}(edta)] and HO_2.[20] Since a similar pH dependence is observed for both reaction steps under conditions of excess [Fe^{II}(edta)] in the present study, we now prefer to interpret the observed catalytic effect of H^+ in terms of the protonation of [Fe^{II}(edta) H_2O]$^{2-}$ and the changeover in geometry as described above.

$$\underset{\text{MCP}}{[Fe^{II}(edta)(H_2O)]^{2-}} + H^+ \overset{K_1}{\rightleftharpoons} \underset{\text{PB}}{[Fe^{II}(edtaH)(H_2O)]^-} \quad (1a)$$

$$\underset{\text{PB}}{[Fe^{II}(edtaH)(H_2O)]^-} + H^+ \overset{K_1'}{\rightleftharpoons} \underset{\text{MCP}}{[Fe^{II}(edtaH_2)(H_2O)]} \quad (1b)$$

All three complexes can react with O_2 to produce [Fe^{II}(edta)O_2]$^{2-}$ and [Fe^{II}(edtaH)O_2]$^{-}$, respectively, as shown in (2). These reactions are substitution-controlled equilibria,

$$[Fe^{II}(edta)(H_2O)]^{2-} + O_2 \overset{K_2}{\rightleftharpoons} [Fe^{II}(edta)(O_2)]^{2-} + H_2O \quad (2a)$$

$$[Fe^{II}(edtaH)(H_2O)]^- + O_2 \overset{K_2'}{\rightleftharpoons} [Fe^{II}(edtaH)(O_2)]^- + H_2O \quad (2b)$$

$$[Fe^{II}(edtaH_2)(H_2O)] + O_2 \overset{K_2''}{\rightleftharpoons} [Fe^{II}(edtaH_2)(O_2)] + H_2O \quad (2c)$$

in which the protonated pentagonal-bipyramidal species can bind O_2 more rapidly than the nonprotonated and diprotonated monocapped trigonal-prismatic species. These reactions are suggested to account for the very fast initial reaction step, not resolvable under most reaction conditions. Substitution of coordinated H_2O by O_2 in the [Fe^{II}(edta)] complexes is not

(27) Clark, N. H.; Martell, A. E. *Inorg. Chem.* **1988**, *27*, 1297.
(28) Anderegg, G. In *Comprehensive Coordination Chemistry*; Wilkinson, G., Gillard, R. D., McCleverty, J. A., Eds.; Pergamon: New York, 1987; Vol. 2, p 777.
(29) Marton, A.; Süksösd-Rozlosnik, N.; Vertes, A.; Nagy-Czako, I.; Burger, K. *Inorg. Chim. Acta* **1987**, *137*, 173.
(30) Whidbey, J. F.; Leyden, D. E. *Anal. Chim. Acta* **1970**, *51*, 25.
(31) Manley, C. *Z. Angew. Phys.* **1971**, *32*, 187.
(32) Bloch, J.; Navon, G. *J. Inorg. Nucl. Chem.* **1980**, *42*, 693.
(33) Oakes, J.; Smith, E. G. *J. Chem. Soc., Faraday Trans. 1* **1983**, *79*, 543.
(34) Kanamori, K.; Dohniwa, H.; Ukita, N.; Kanesaka, I.; Kawai, K. *Bull. Chem. Soc. Jpn.* **1990**, *63*, 1447.
(35) Kennard, C. H. L. *Inorg. Chim. Acta* **1967**, *1*, 347.
(36) Solans, X.; Font Alba, M. *Acta Crystallogr.* **1984**, *C40*, 635.
(37) Mizuta, T.; Yamamoto, T.; Miyoshi, K.; Kushi, Y. *Inorg. Chim. Acta* **1990**, 121.

expected to cause a significant UV−vis spectral change. The subsequent redox reactions (3), which produce superoxo com-

$$[Fe^{II}(edta)(O_2)]^{2-} \xrightarrow{k_3} [Fe^{III}(edta)(O_2^-)]^{2-} \quad (3a)$$

$$[Fe^{II}(edtaH)(O_2)]^{-} \xrightarrow{k_3'} [Fe^{III}(edtaH)(O_2^-)]^{-} \quad (3b)$$

$$[Fe^{II}(edtaH_2)(O_2)] \xrightarrow{k_3''} [Fe^{III}(edtaH_2)(O_2^-)] \quad (3c)$$

plexes of [Fe^{III}(edta)], will induce a significant spectral change and are suggested to account for the first reaction step for which complete kinetic data could be recorded. Thus electron transfer is the rate-determining step following the rapid coordination of O_2 in (2). The observed rate constant, k_{obs2}, is expected to depend on pH since the various species produced in (2) are expected to undergo oxidation at different rates.

The given rate law (4), derived under conditions where [Fe^{II}(edta)] >> [O_2], can account for the sigmoid-shaped pH dependence observed at pH ≥ 2.5 in Figure 2.

$$k_{obs2} = \left\{\frac{k_3K_2 + k_3'K_2'K_1[H^+] + k_3''K_2''K_1'K_1[H^+]^2}{1 + K_1[H^+] + K_1K_1'[H^+]^2}\right\}[Fe^{II}(edta)] \quad (4)$$

The rate constant of the subsequent reaction step, k_{obs3}, exhibits a similar pH profile (Figure 2) and is on the average ca. 2 times smaller than k_{obs2}. Since these experiments are performed in the presence of excess [Fe^{II}(edta)], we suggest that equilibrium 1 must also account for the pH dependence found for this reaction step. Thus the superoxo species produced in (3) may react further as shown in (5). The rate law for these reactions will be similar to (4), as summarized in (6).

$$[Fe^{III}(edta)(O_2^-)]^{2-} + [Fe^{II}(edta)(H_2O)]^{2-} \xrightarrow{k_4} [(edta)Fe^{III}(O_2^{2-})Fe^{III}(edta)]^{4-} + H_2O \quad (5a)$$

$$[Fe^{III}(edtaH)(O_2^-)]^{-} + [Fe^{II}(edtaH)(H_2O)]^{-} \xrightarrow{k_4'} [(edtaH)Fe^{III}(O_2^{2-})Fe^{III}(edtaH)]^{2-} + H_2O \quad (5b)$$

$$[Fe^{III}(edtaH_2)(O_2^-)] + [Fe^{II}(edtaH_2)(H_2O)] \xrightarrow{k_4''} [(edtaH_2)Fe^{III}(O_2^{2-})Fe^{III}(edtaH_2)] + H_2O \quad (5c)$$

$$k_{obs3} = \left\{\frac{k_4 + k_4'K_1[H^+] + k_4''K_1K_1'[H^+]^2}{1 + K_1[H^+] + K_1K_1'[H^+]^2}\right\}[Fe^{II}(edta)] \quad (6)$$

The [Fe^{II}(edta)] dependence of k_{obs} was studied at pH ∼ 2.5 and 6, at the maximum and the minimum of the pH-dependence plots, respectively, as shown in Figure 2. The values of k_{obs} for all three reaction steps varied linearly with [Fe^{II}(edta)] over a limited concentration range (see typical examples in Figure 3). The linear concentration dependence observed for k_{obs2} indicates that the equilibria in (2) are unfavorable since larger binding constants would result in a nonlinear concentration dependence. The lability of coordinated water and oxygen in (2) is expected to be high (see further discussion), such that the unfavorable binding constant must be related to the unfavorable concentration ratio of oxygen and water. At higher concentrations, the dependencies deviate from linearity, suggesting a higher order dependence on [Fe^{II}(edta)]. This is presumably due to the kinetic overlap of the subsequent reactions through

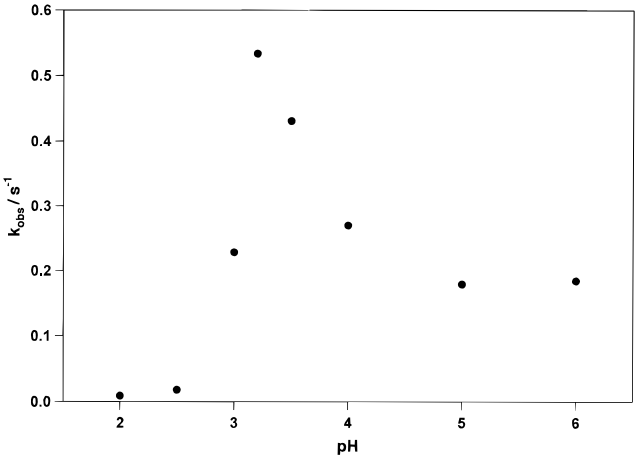

Figure 4. pH dependence of k_{obs2} (●) for the oxidation of [Fe^{II}(edta)] in the presence of an excess of O_2. Experimental conditions: [O_2] = 6.25×10^{-4} M, [Fe^{II}(edta)] = 3.0×10^{-5} M, ionic strength = 0.5 M, [acetate buffer] = 0.1 M for pH > 3, T = 25 °C, λ = 260 nm.

which a higher order dependence on [Fe^{II}(edta)] can occur. The preceding simplified treatment only valid when the different reaction steps can be separated as described above. At pH = 2.2, where all three reaction steps could be resolved, the second-order rate constants are $k_1 = 22\,000 \pm 2000$ M^{-1} s^{-1}, $k_2 = 4000 \pm 300$ M^{-1} s^{-1}, and $k_3 = 2130 \pm 80$ M^{-1} s^{-1} at 25 °C, which correspond to the reaction steps outlined in (2), (3), and (5), respectively.

Reactions in the presence of an excess of oxygen only revealed one kinetic step which exhibited good first-order behavior between pH = 6 and pH = 4. At lower pH values, the fit of the absorbance vs time trace with one exponential function was no longer perfect. Furthermore, an additional fast step, with a small increase in absorbance, could be observed at pH = 3.2; viz., $k_{obs} = 30$ s^{-1}. This step may be related to ring opening of the protonated form which occurs when oxygen enters the coordination sphere of the complex. This explanation seems to be feasible, especially since the fast step cannot be resolved at pH < 2.5, where the diprotonated less reactive species in solution becomes dominant. The studied pH dependence exhibits a maximum at pH = 3 (see Figure 4) and is in close agreement with the pH dependence found in an excess of [Fe^{II}(edta)] (see Figure 2). The small shift in the maximum can be explained by the much lower complex concentration, which affects the distribution of species in solution. The [O_2]-dependence data obtained under such conditions at pH = 6, are summarized in Figure 5, from which it follows that the reaction with O_2 is an equilibrium process. The slope of the line, viz. 266 ± 7 M^{-1} s^{-1}, is very close to that observed for the second reaction step in the presence of excess [Fe^{II}(edta)]; viz., $k_2 = 286 \pm 24$ M^{-1} s^{-1} under similar conditions. The overall equilibrium constant for the binding of O_2 and formation of [Fe^{III}(edta)(O_2^-)]$^{2-}$ is ca. 10^4 M^{-1} based on the data of Figure 6. This equilibrium constant cannot be compared directly with the data in Figure 4, since the intercept for the k_{obs2} data has a large error limit.

The temperature and pressure dependencies of the reactions were studied in the presence of excess [Fe^{II}(edta)]. Typical plots to illustrate the effect of pressure on k_{obs2} and k_{obs3} are presented in the Supporting Information (Figure S3). The obtained activation parameters are summarized in Table 1.

Decomposition Reactions. During most measurements, the obtained [Fe^{III}] product was observed to decompose very slowly. This was also noticed previously by Wubs et al.[10] Measurements with the rapid-scan equipment at a longer reaction time clearly show the slow decomposition process (see Supporting

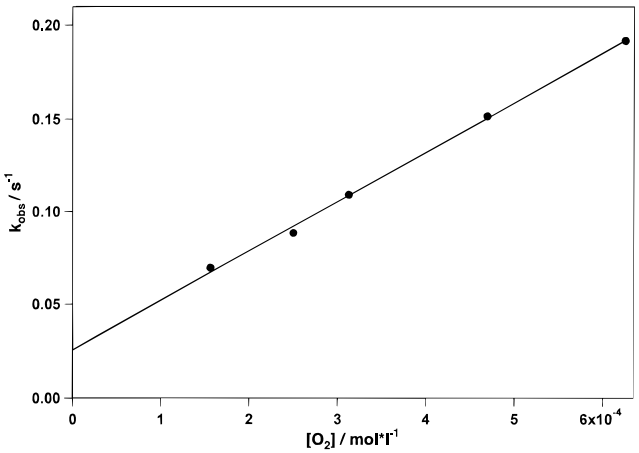

Figure 5. k_{obs2} (●) as a function of [O_2] for the oxidation of [Fe^{II}(edta)]. Experimental conditions: [Fe^{II}(edta)] = 3.0×10^{-5} M, ionic strength = 0.5 M, [acetate buffer] = 0.1 M, pH = 6, T = 25 °C, λ = 260 nm.

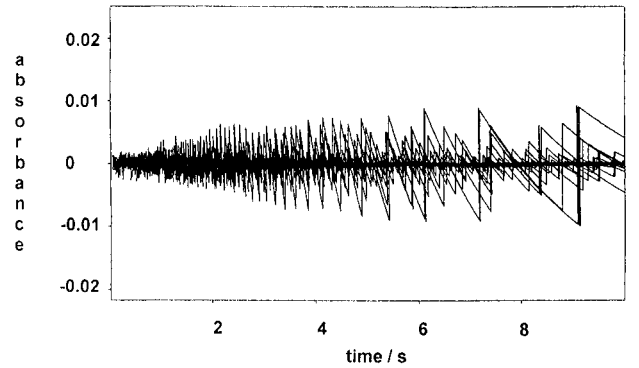

Figure 6. Typical fit with four exponential functions. Experimental conditions: [Fe^{II}(edta)] = 2.5×10^{-3} M, [O_2] = 1.25×10^{-4} M, ionic strength = 0.5 M, [acetate buffer] = 0.1 M for pH = 6, T = 25 °C, optical path length = 0.2 cm, Δt = 10 s.

Table 1. Summary of Rate and Activation Parameters for the Oxidation of [Fe^{II}(edta)] by Molecular Oxygen[a]

pH	k_2 (M^{-1} s^{-1}) T = 25 °C	$\Delta H_2^{\ddagger}$ (kJ mol^{-1})	$\Delta S_2^{\ddagger}$ (J mol^{-1} K^{-1})	$\Delta V_2^{\ddagger}$ (cm^3 mol^{-1})
6	320 ± 25	50 ± 2	−30 ± 7	−16.1 ± 1.6
2.5	2472 ± 244	42 ± 2	−40 ± 8	
pH	k_3 (M^{-1} s^{-1}) T = 25 °C	$\Delta H_3^{\ddagger}$ (kJ mol^{-1})	$\Delta S_3^{\ddagger}$ (J mol^{-1} K^{-1})	$\Delta V_3^{\ddagger}$ (cm^3 mol^{-1})
6	133 ± 11	45 ± 1	−53 ± 4	−16.2 ± 2.5
2.5	1428 ± 164	43 ± 3	−41 ± 11	

[a] Experimental conditions: [Fe^{II}] = 2.5 mM, [O_2] = 0.125 mM, ionic strength = 0.5 M, [acetate buffer] = 0.1 M (pH >3), λ = 370 nm.

Information (Figure S4)). It was not possible to study the decomposition quantitatively, since it did not seem to follow clean first-order kinetics. However, the observed rate constant is of the order of $k_{obs} = 10^{-3}$ s^{-1} for [Fe^{II}] = 2.5 mM, [O_2] = 0.13 mM, pH = 6, and I = 0.5 M. We believe that the observed decomposition reaction can be ascribed to photochemical effects since the reaction seems to depend on the light intensity and wavelength used to monitor the reaction. The photochemical activity of this system has also been noted in the literature.[38]

EPR Experiments. EPR experiments were performed with ATBS [2,2′-azinobis(3-ethyl-2,3-dihydrobenzthiazole-6-sulfonate)] as a radical scavenger to investigate whether reactive intermediates or side products (hydroxyl radicals, superoxide or peroxide ions, or Fe^{IV}edta) are formed in the reaction mixture.[9] The [Fe^{II}(edta)] solution that contained ATBS was oxidized with air and immediately frozen in liquid nitrogen. A color change from colorless to yellow was observed. EPR spectra were recorded at 75 K, and only a sharp peak at g = 4.3 was detected (see Supporting Information (Figure S5)). By way of comparison, the [Fe^{II}(edta)] solution was oxidized with H_2O_2. The resulting green solution showed an absorbance maximum at 660 nm in the UV−vis spectrum, which corresponds to the $ATBS^+$ cation. This sample was measured at 75 K and showed a strong peak at g = 2, which further indicates the formation of the $ATBS^+$ cation (see Supporting Information (Figure S6)). In both spectra, another peak at g = 4.3, belonging to the monomer [Fe^{III}(edta)H_2O][29] (see Supporting Information (Figure S7)), was observed. The EPR spectra clearly show that no radicals were formed during the investigated reaction. Under the same conditions, the band at 660 nm in the UV−vis spectrum was also not detected.

Overall Suggested Mechanism. At least three reaction steps could be resolved during the interaction of dioxygen with an excess of [Fe^{II}(edta)]. These include the stepwise substitution of a coordinated water molecule by dioxygen, followed by an intramolecular electron-transfer reaction to produce an Fe^{III}−superoxo complex, which in the third step reacts with another [Fe^{II}(edta)] species to produce a dimeric [Fe^{III}−O_2^{2-}−Fe^{III}] complex, which dissociates rapidly to form the monomeric [Fe^{III}(edta)] complex. In principle, it should be possible to observe four reaction steps, of which two are associated with substitution and electron transfer of the first [Fe^{II}(edta)] complex and two are associated with similar reactions of the second [Fe^{II}(edta)] complex. With the aid of a global analysis program, it was possible to fit the kinetic data to a four-step mechanism (see typical fit in Figure 6), whereas only three steps could be resolved precisely. The four rate constants, which were obtained with the aid of this program are k_1 = 14 000 ± 4000 M^{-1} s^{-1}, k_2 = 264 ± 23 M^{-1} s^{-1}, k_3 = 13 000 ± 2000 M^{-1} s^{-1}, and k_4 = 166 ± 8 M^{-1} s^{-1} for pH = 6 with [Fe^{II}(edta)] in excess. The four reaction steps referred to above all exhibit a linear dependence on [Fe^{II}(edta)], from which the second-order rate constants were calculated. This means that the substitution equlibria for the first and third steps must be unfavorable in order to result in a concentration dependence of the second and fourth reaction steps. k_1 is so large that it could not be determined accurately by stopped-flow techniques. This is in close agreement with rate constants obtained by other investigators for the first step; e.g., Purmal et al.[5] have reported a value of $k_1 = 2.3 \times 10^3$ M^{-1} s^{-1}.

The intermediate H_2O_2 formed could not be detected by the reaction with titanyl sulfate, and it could be shown above that no radicals are formed. We therefore conclude that the produced H_2O_2 reacts rapidly with the excess of [Fe^{II}(edta)] to form the monomeric [Fe^{III}(edta)] complex and water. We remeasured the rate constant of this process and found it to be 1.78×10^4 M^{-1} s^{-1} at pH = 6 and T = 25 °C, which is in very close agreement with values reported in the literature.[9,39] This rapid subsequent reaction also accounts for the fact that no evidence for the participation of radicals under these conditions could be found.

The extinction coefficient of [Fe^{II}(edta)] at pH = 6 was found to be 1180 M^{-1} cm^{-1} at 260 nm, and the extinction coefficient of [Fe^{III}(edta)] under similar conditions was found to be 7735 M^{-1} cm^{-1}.[40] From these extinction coefficients, it could be shown that the final spectrum belongs to the monomeric [Fe^{III}(edta)] complex and that the stoichiometry of the reaction

(38) Lunak, S.; Sedlak, P. *J. Photochem. Photbiol. A: Chem.* **1992**, *68*, 1.
(39) Borggard, O. K.; Farver, O.; Andersen, V. S. *Acta Chem. Scand.* **1971**, *25*, 3541.
(40) Sörensen, M.; Frimmel, F. H. *Z. Naturforsch.* **1995**, *50B*, 1845.

Table 2. Comparison of Available Literature Data for the Kinetics of [Fe^{II}(edta)] Oxidation by Dioxygen

obsd reacn step	rate constant $T = 25$ °C	$\Delta H^{\ddagger}$ (kJ mol^{-1})	$\Delta S^{\ddagger}$ (J mol^{-1} K^{-1})	$\Delta V_2^{\ddagger}$ (cm^3 mol^{-1})	exptl conditions	order in Fe^{II}	order in O_2	ref
one	20 M^{-1} s^{-1}				pH = 6, Fe^{II} in excess	1	1	Brown et al.[7]
one	270 M^{-1} s^{-1}				oxygen in excess	1	1	Kurimura et al.[4]
one	1×10^{10} M^{-1} s^{-1} ($T = 22$ °C)				pH = 4, oxygen excess	1	1	Purmal et al.[5]
one	0.9 $dm^{1.6}$ $mol^{-0.54}$ s^{-1}	20.8			pH = 6−8, Fe^{II} in excess	1	0.5	Sada et al.[6]
one	6.52×10^3 M^{-2} s^{-1}	24.7			pH = 7.5, Fe^{II} in excess	2	1	Wubs et al.[10]
one	187 ± 3 M^{-1} s^{-1}	47.6 ± 0.6	-91 ± 2	-16.9 ± 1.2	pH = 5, Fe^{II} in excess	1	1	Zang et al.[20]
one	1.87×10^4 M^{-2} s^{-1}	33.9 ± 1.4	-115 ± 4	-12.7 ± 0.9	pH = 5, Fe^{II} in excess	2	1	Zang et al.[20]
one	302 ± 8 M^{-1} s^{-1}				pH = 6, oxygen in excess	1	1	Zang et al.[20]
one	286 ± 24 M^{-1} s^{-1}	50 ± 2	-30 ± 7	-16.1 ± 1.6	pH = 6, Fe^{II} in excess	1	1	this study
two	161 ± 7 M^{-1} s^{-1}	45 ± 1	-53 ± 4	-16.2 ± 2.5	pH = 6, Fe^{II} in excess	1	1	this study
one	266 ± 7 M^{-1} s^{-1}				pH = 6, oxygen in excess	1	1	this study

is close to 4:1 (Fe:O_2), which corresponds to our postulation that only monomeric [Fe^{III}(edta)] and water are formed as final products.

The rate constants clearly show that the substitution processes are very fast and are followed by the rate-determining electron-transfer processes. This is one of the reasons that we were unable to detect the postulated intermediates as the superoxo or peroxo species, because they immediately react once they are formed. Furthermore, the characteristic bands for the $[Fe^{III}(edta)O_2]^{2-}$ complex at 287 nm ($\epsilon = 6100$ M^{-1} cm^{-1}) and 520 nm ($\epsilon = 530$ M^{-1} cm^{-1}) show in comparison to that for $[Fe^{III}(edta)H_2O]^-$ with $\epsilon = 9290$ M^{-1} cm^{-1} (256 nm)[15,16,41] low extinction coefficients, such that the spectra of the intermediates would be hidden by the product spectrum.

The reaction with dioxygen is controlled by ligand substitution in the $[Fe^{II}(edta)H_2O]^{2-}$ complex. Since this complex is a seven-coordinate (20-electron) species, it is realistic to assume that the substitution of coordinated water by dioxygen follows a dissociative path. The subsequent slower intramolecular electron-transfer process (reaction 3) must be controlled by a reorganization barrier in order to convert [Fe^{II}−O_2] to [Fe^{III}−O_2^-]. This reaction is characterized by significantly negative $\Delta S^{\ddagger}$ and $\Delta V^{\ddagger}$ values (Table 1), which must be related to the oxidation of Fe^{II} to Fe^{III} and the reduction of O_2 to O_2^-. Both of these processes are expected to involve a significant decrease in partial molar volume and an increase in electrostriction.[42−44] The efficiency of the ligand substitution process is controlled by the nature of the $[Fe^{II}(edta)H_2O]^{2-}$ complex, which on protonation produces a more labile $[Fe^{II}(edtaH)H_2O]^-$ species. The latter accounts for the drastic increase in observed rate constant on decreasing the pH in the range pH 5−3.

The reaction of the second $[Fe^{II}(edta)H_2O]^{2-}$ species results in very similar concentration, pH, temperature, and pressure dependencies, which are once again interpreted in terms of a rapid complex-formation reaction followed by a rate-determining electron-transfer process. This reaction is once again characterized by significantly negative $\Delta S^{\ddagger}$ and $\Delta V^{\ddagger}$ values for the same reasons as outlined above. A summary of the available literature data is given in Table 2. A comparison with the data reported in our earlier study,[20] in which only one reaction step could be resolved, shows good agreement with the second step observed in the present study in terms of the second-order rate constant and the associated activation parameters (especially $\Delta S^{\ddagger}$ and $\Delta V^{\ddagger}$). The very similar activation parameters observed for both oxidation processes indicate that a similar reorganization barrier must exist. When oxygen is used in excess, only one reaction step is observed between pH = 4 and pH = 6 since a peroxo-bridged complex cannot be formed under these conditions. This is in good agreement with the second reaction step observed in the presence of an excess of [Fe^{II}(edta)]. Again the reaction is controlled by electron transfer and the associated reorganization barrier. At lower pH, a second fast process occurs, which may be related to ring opening of the edta ligand when dioxygen enters the coordination sphere. Moreover, the rate of this step decreases at pH ≤ 2.5 since the diprotonated species becomes dominant and is less reactive.

Scheme 1

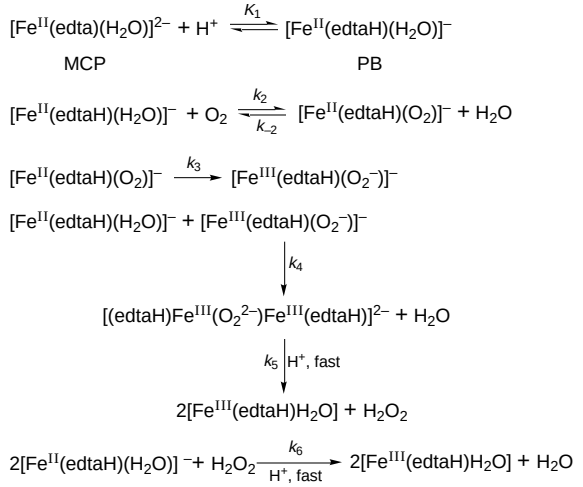

The results of this study have clearly shown that the improved rapid-scan techniques as well as the more sophisticated data analysis programs reveal significantly more details concerning the various reaction steps in the autoxidation [Fe^{II}(edta)]. We are now able to suggest a detailed multistep mechanism as shown in Scheme 1. At high pH (pH = 6), mostly the nonprotonated form will react whereas, at low pH (pH ≤ 4), the more reactive monoprotonated form will react. The mechanism in Scheme 1 is given for the more reactive protonated species.

Acknowledgment. The authors gratefully acknowledge financial support from the Deutsche Forschungsgemeinschaft and the Volkswagen-Stiftung. They also appreciate the help of Dr. Ralf Alsfasser with the EPR measurements.

Supporting Information Available: Typical rapid-scan spectra of the investigated reaction, a distribution diagram of the [Fe^{II}(edta)] species in solution, plots of ln k_{obs2} and ln k_{obs3} vs pressure, rapid-scan spectra of the decomposition reaction, and EPR spectra of [Fe^{III}(edta)] in the presence and absence of the used radical scavenger (9 pages). Ordering information is given on any current masthead page.

IC970158T

(41) Francis, K. C.; Cummnis, D.; Oakes, J. *J. Chem. Soc., Dalton Trans.* **1985**, 493.
(42) van Eldik, R.; Asano, T.; le Noble, W. J. *Chem. Rev.* **1989**, *89*, 549.
(43) Zhang, M.; van Eldik, R.; Espenson, J. H.; Bakac, A. *Inorg. Chem.* **1994**, *33*, 130.
(44) Projahn, H.-D.; Schindler, S.; van Eldik, R.; Fortier, D. G.; Andrew, C. R.; Sykes, A. G. *Inorg. Chem.* **1995**, *34*, 5935.